Met. Mater. Int., Vol. 15, No. 5 (2009), pp. 741~751
doi: 10.1007/s12540-009-0741-5 Published 26 October 2009

The Dependence of Lamellar Spacings and Microhardness on the Growth Rate in the Directionally Solidified Bi-43 wt.% Sn Alloy at a Constant Temperature Gradient

E. Çadırlı[1,*], H. Kaya[2], and N. Maraşlı[3]

[1]Department of Physics, Faculty Arts & Sciences, Niğde University, Niğde, Turkey
[2]Department of Science Education, Education Faculty, Erciyes University, 38039 Kayseri-Turkey
[3]Department of Physics, Faculty Arts & Sciences, Erciyes University, 39039, Kayseri- Turkey

(received date: 13 January 2008 / accepted date: 7 January 2009)

Bi-43 wt.% Sn eutectic samples were directionally solidified upward with five different growth rates (V = 8.3-164.8 μm/s) at a constant temperature gradient (G = 3.55 K/mm) in a Bridgman type directional solidification furnace. The lamellar spacings (λ) and microhardness values (H_V) were measured from the quenched samples; the directionally solidified Bi-43 wt.% Sn eutectic alloy and the minimum undercoolings (ΔT) were determined from the Jackson–Hunt eutectic theory. The dependency of lamellar spacings (λ), microhardness (H_V) and undercooling (ΔT) on the growth rate (V) were analyzed. According to these results, it has been found that the value of λ decreases with the increasing value of V and that the values of H_V and ΔT increase for a constant G. The values of $\lambda^2 V$, $\lambda\Delta T$ and $\Delta T\ V^{0.5}$ were determined by using the values of λ, ΔT and V. The results obtained in the present work have been compared with those predicted by the Jackson–Hunt eutectic theory and with similar experimental results.

Keywords: metals and alloys, directional solidification, mechanical properties, microstructure

1. INTRODUCTION

Eutectic alloys are the basis of many engineering materials [1-4]. Thus, the eutectic microstructure and the relationship between the microstructure and the solidification conditions have been studied extensively for both scientific and technological reasons [5-34]. This kind of microstructure is a classic example of spontaneous two-phase pattern formation in nature, and has important applications as an in-situ grown composite material. Eutectic growth involves the interacting nucleation and cooperative growth of two or more solid phases within one liquid phase. A general model for eutectic growth was first developed by Jackson and Hunt (JH) [11] for eutectic growth in eutectic as well as off-eutectic alloy compositions. The result of this model was examined to obtain relationships between eutectic spacing, interface undercooling and growth rate.

From an experimental point of view, different eutectic microstructures have been found and have been classified as regular lamellar, regular rod eutectic, and irregular or anomalous eutectic. Directional solidification of binary or pseudo-binary eutectics may result in regular structures of fibrous or lamellar type. When two solid phases (α and β) grow from a liquid of eutectic composition C_E, the average undercooling, ΔT at the interface results from three contributions and can be expressed as

$$\Delta T = T_E - T_L = \Delta T_s + \Delta T_r + \Delta T_k \quad (1)$$

where T_E is the eutectic melting temperature and T_L is the local interface temperature; ΔT_s is the solute undercooling, ΔT_r is the curvature undercooling and ΔT_k is the kinetic undercooling. For regular metallic eutectic systems, however, ΔT_k can usually be ignored compared with ΔT_c and ΔT_r, which are equal for eutectic growth at the extremum [11].

The Jackson-Hunt (J-H) eutectic theory [11] gives the following relationship between the undercooling (ΔT), the growth rate (V) and the lamellar spacing (λ) for an isothermal solidification front as

$$\Delta T = K_1\ V\lambda + K_2/\lambda \quad (2)$$

*Corresponding author: ecadirli@gmail.com

where K_1 and K_2 can be calculated from the phase diagram and thermodynamic data and are expressed as

$$K_1 = \frac{mPC_o}{f_\alpha f_\beta D} \quad (3)$$

$$K_2 = 2m\delta\left(\frac{\Gamma_\alpha \sin\theta_\alpha}{m_\alpha f_\alpha} + \frac{\Gamma_\beta \sin\theta_\beta}{m_\beta f_\beta}\right) \quad (4)$$

where $m = m_\alpha m_\beta/(m_\alpha + m_\beta)$ in which m_α and m_β are the slopes of the liquidus lines of the α and β phases at the eutectic temperature, C_o is the composition difference between the α and the β phases, f_α and f_β are the volume fractions of α and β phases, respectively, Γ_α and Γ_β are the Gibss-Thomson coefficients of α and β phases, respectively, D is the solute diffusion coefficient for the melt, θ_α and θ_β are the groove angles of α/liquid phases and β/liquid phases at the three-phase conjunction point, P is the Peclet number and δ is the growth parameter. These thermodynamic data [15,35-39] concerning Sn-Bi eutectic alloy are given in Table 1. The parameter δ is unite for the lamellar growth and the Peclet number (P) for lamellar eutectic growth is defined as [11],

$$P = 0.3383(f_\alpha f_\beta)^{1.661} \quad (5)$$

Investigation of Eq. 2 gives the relationship between the extremum lamellar spacing (λ_e) growth rate (V) and undercooling (ΔT) as,

$$\lambda_e^2 V = K_2/K_1 \quad (6(a))$$

$$\Delta T_m \lambda_e = 2K_2 \quad (6(b))$$

$$\frac{\Delta T_m^2}{V} = 4K_1K_2 \quad (6(c))$$

Table 1. The some physical parameters for Bi- 43 wt.% Sn eutectic alloy

Properties	Values
T_E (K)	412 [35]
m_α K(% wt.)$^{-1}$	-2.58[36]
m_β K(% wt.)$^{-1}$	3.09 [36]
C_E (% wt.)	43[36]
C_o (% wt.)	78.9[36]
f_α (-)	0.543 [36]
f_β (-)	0.467 [36]
Γ_α (K.μm)	0.102 [37]
Γ_β (K.μm)	0.105 [38]
θ_α (^{o})	35.0 [15]
θ_β (^{o})	37.88 [38]
D (μm^2/s)	1600 [39]
K_1 (K s/μm^2)	0.0278*
K_2 (μm K)	0.717*
$\lambda^2 V = \frac{K_2}{K_1}(\mu m^3/s)$	25.80*

*calculated from the physical parameters

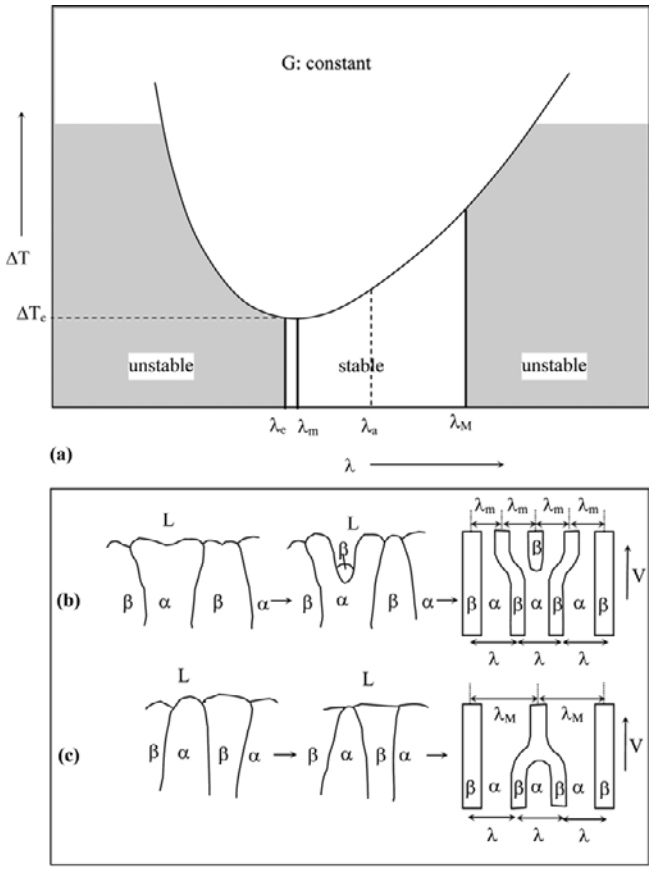

Fig. 1. (a) Schematic plot of average undercooling ΔT versus lamellar spacing l for a given growth rate V. The stable and unstable regions, as predicted by the Jackson-Hunt theory (b) Readjustment of local spacing by the positive terminations. (c) The readjustment of local spacing by the negative terminations.

where λ_e is the extremum lamellar spacing and ΔT_m is the minimum undercooling. A well known conjecture of this criterion is the minimum undercooling argument. This indicates that the spacing λ, as indicated in Fig. 1, will be the operating point of the spacing selection [25]. Although the extremum condition has been confirmed as equivalent to the marginal stability criterion [40], experimental investigations [17,18] have shown that there is no sharp selection criterion for eutectic lamellar spacings.

The experimentally confirmed inter-relationship between the lamellar spacing (λ), the growth rate (V) and the undercooling (ΔT) in a eutectic system implies that a mechanism is available for changing the lamellar spacing when the growth rate and/or undercooling vary. Figure 1(a) shows the variation of the undercooling with lamellar spacing according to the minimum undercooling criterion. As shown in Fig. 1, λ_e is the extremum lamellar spacing, λ_m is the minimum lamellar spacing, λ_M is the maximum lamellar spacing and λ_a is the average lamellar spacing. λ_e is obtained from Eq. 6(a) to (c) and the λ_m, λ_M, λ_a, and λ_e were measured on the trans-

verse section of the samples. When λ is smaller than λ_e, the growth will be unstable and when λ is smaller than λ_m, an overgrowth occurs as shown in Fig. 1(b). When λ becomes greater than λ_M, tip splitting also occurs, as shown in Fig. 1(c) [9]. So lamellar spacings for the steady growth must satisfy $\lambda_m<\lambda_a<\lambda_M$ conditions. For eutectic growth, the ΔT-V-λ relationships can be predicted by the Jackson-Hunt (J-H) [11] and Trivedi-Magnin-Kurz (TMK) [12] theories. The maximum spacing for lamella can be treated by examining the time-dependent growth of a single cell. It was found that maximum stable spacing for lamella was close to the maximum steady-state and that the maximum spacing must be greater than twice the minimum spacing ($\lambda_M \geq 2\lambda_m$), otherwise the new lamella cannot catch up [9].

It is well known that some important solidifcation parameters, such as growth rate, significantly affect the microstructural scale as well as the mechanical properties of metals. Materials processed via directional solidification tend to show advantages of refined micro-structure, reduced microsegregation, etc. [41,42]. Because the mechanical properties of a material depend largely on its microstructure, controlled formation of such microstructures is essential to develop new materials with desired properties [43-46].

The mechanical properties, i.e. microhardness (H_V) of the directional solidified materials, also depend on the solidification parameters, i.e. the growth rates (V). The relationships among the microhardness (H_V), the growth rate (V) and lamellar spacings (λ) can be expressed on logarithmic scales. The Hall-Petch type relationships can be written as follows [47,48]:

$$H_V = k_1 V^m \tag{7}$$

$$H_V = k_2 \lambda^{-n} \tag{8}$$

where m and n are exponent values for the growth rate and the lamellar spacing, respectively, and k_1 and k_2 are the constants that can be determined experimentally.

Accordingly, the purposes of the present work were to investigate the effect of growth rate on the lamellar spacings and microhardness of Bi-Sn eutectic alloy and to compare the results with the previous experimental results and the existing theoretical model. Thus, the composition of Bi-Sn alloy was chosen to be a eutectic composition (Bi-43 wt.% Sn) to observe the lamellar spacings.

2. EXPERIMENTAL PROCEDURE

2.1. Sample production and microstructure observation

The eutectic samples (Bi- 43 wt.% Sn) were prepared by melting the weighed quantities of Sn and Bi of (>99.99 %) high purity metals in a graphite crucible, which was placed into a vacuum melting furnace [23]. After allowing time for melt homogenization, the molten alloy was poured into thirteen graphite crucibles (250 mm in length, 4 mm ID and 6.35 mm OD) which were placed into the hot filling furnace. Then, each sample was positioned in a Bridgman type furnace in a graphite cylinder (300 mm in length, 10 mm ID and 40 mm OD). After stabilizing the thermal conditions in the furnace under an argon atmosphere, the sample was grown by pulling it downwards at various growth rates (8.3 μm/s to 164.8 μm/s, G constant) by means of different speeded synchronous motors. After 100 mm to 120 mm steady state growth of the samples, they were quenched by pulling them rapidly into the water reservoir [49]. After metallographic processes including mechanical and electro polishing techniques, the microstructures of the samples were revealed. The microstructures of the samples were characterized using an LEO scanning electron microscope (SEM) equipped with an energy dispersive X-ray (EDX) spectrometer as well as with a computer controlled image analyzer. Microstructures of the samples were photographed from both transverse and longitudinal sections by means of scanning electron microscopy (SEM). Typical SEM images for different growth rates are shown in Fig. 2. In addition, to designate and make sure of solid phases, quantitative composition analysis of solid lamella phases in the sample was

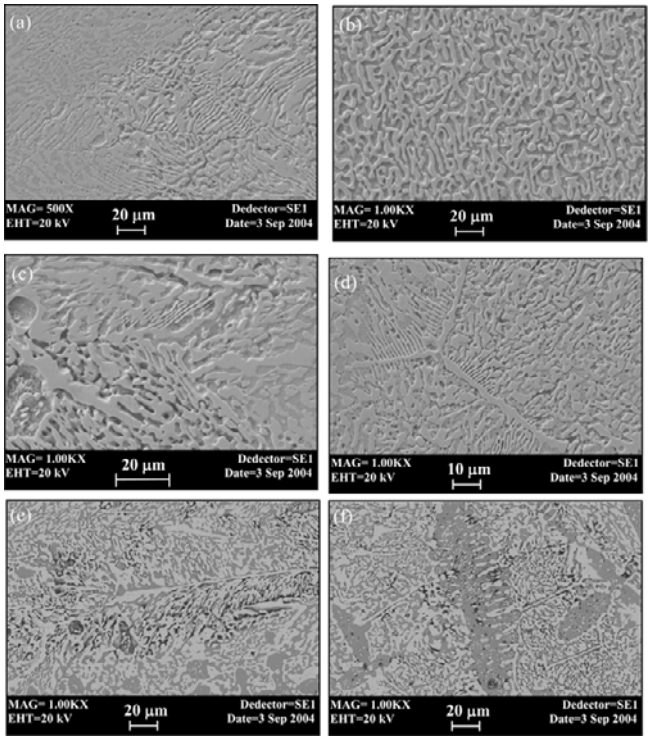

Fig. 2. Some SEM images of the growth morphologies of directionally solidified Bi- 43 wt.% Sn eutectic alloy with different growth rates (8.3 μm/s to 164.8 μm/s) in a constant temperature gradient (G = 3.55 K/mm), (a) longitudinal section (b) transverse section (V = 8.3 μm/s), (c) longitudinal section (d) transverse section (V = 40.2 μm/s), (e) longitudinal section (f) transverse section (V = 164.8 μm/s).

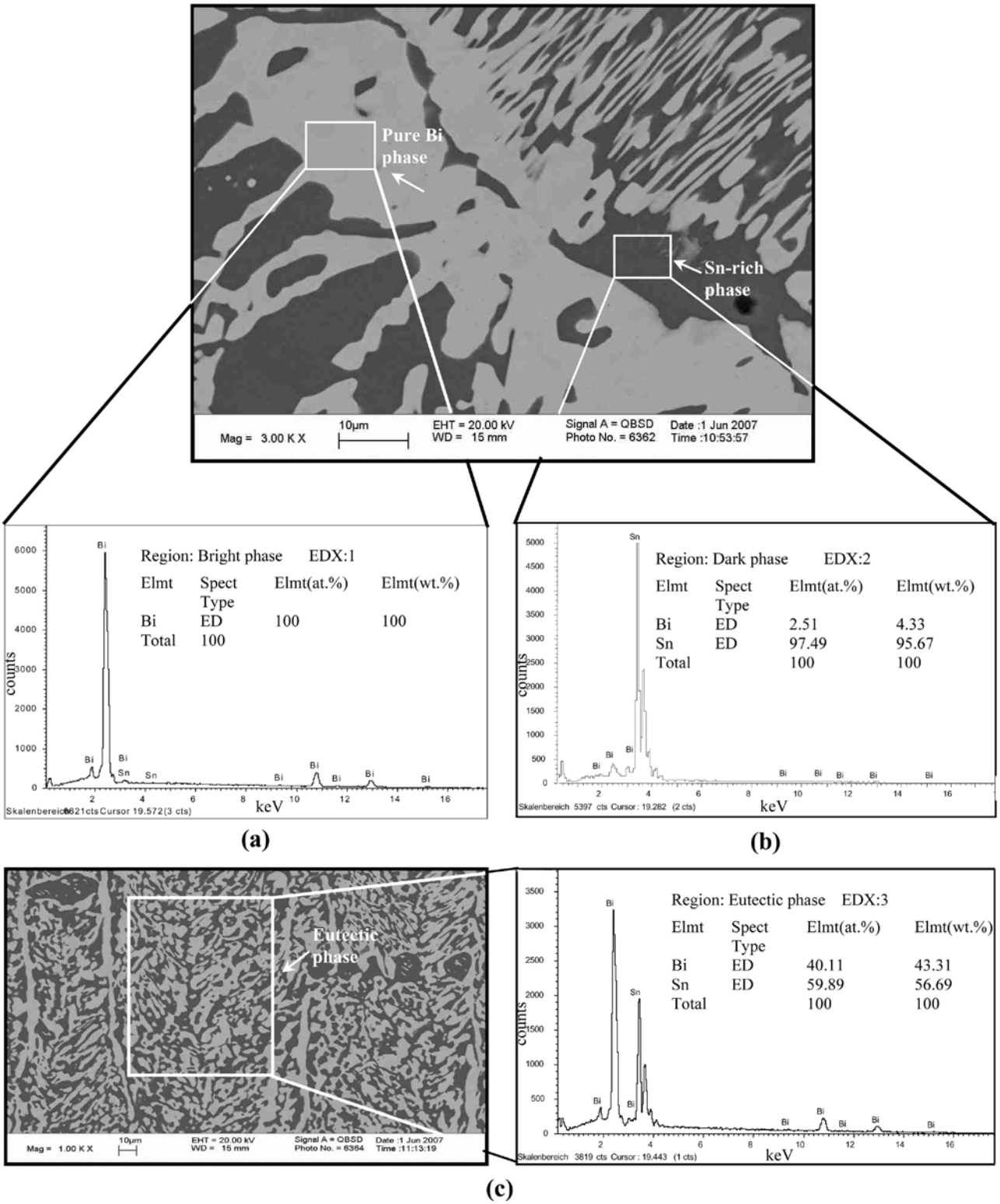

Fig. 3. The composition analysis of the Bi- 43 wt.% Sn eutectic alloy by using SEM EDX (a) Pure Bi (grey phase) (b) Sn-rich phase (dark phase) (c) Lamelllar eutectic structure (homogenous phase).

carried out by using EDX spectrometers, as shown in Fig. 3. The solubility of Bi in Sn and the solubility of Sn in Bi are 2.7 wt.% Bi and less than 0.1 wt.% Sn at room temperature, respectively [50]. According to EDX results and the solubil-

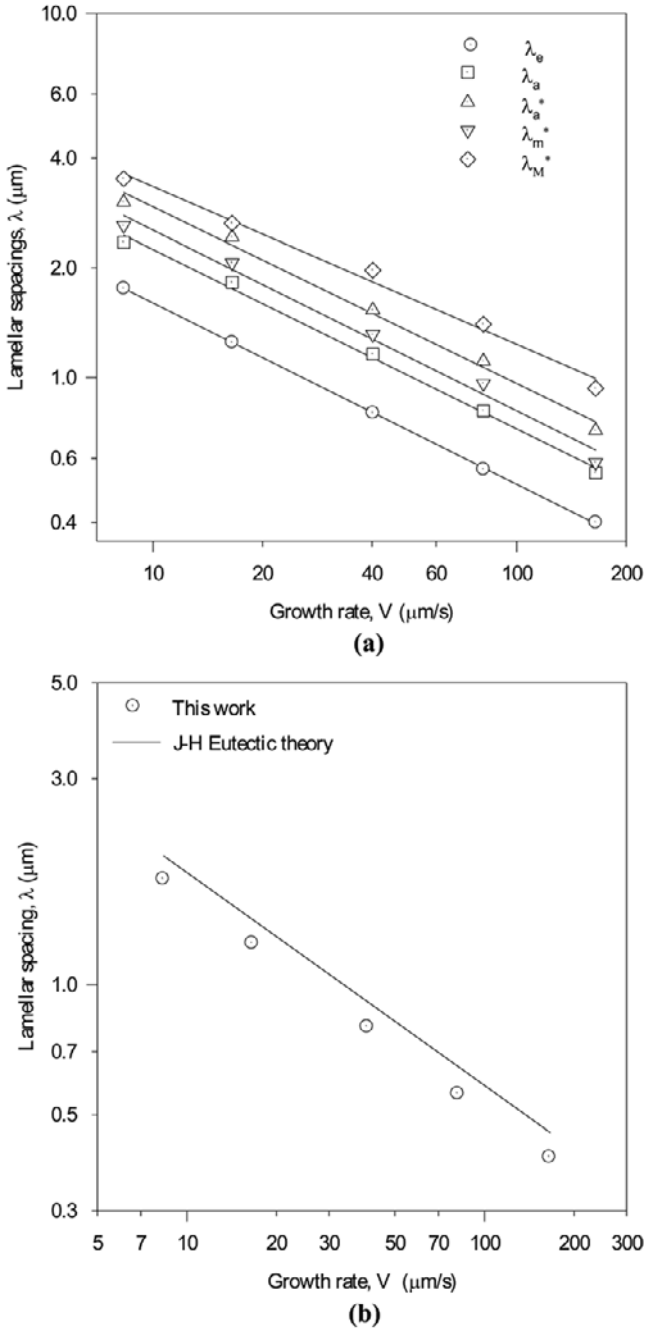

Fig. 4. (a) Variation of lamellar spacings as a function of growth rates (V) at a constant temperature gradient (G = 3.55 K/mm), (b) Comparison of the experimental results obtained in present work with the results of J-H eutectic theory for the Bi- 43 wt.% Sn eutectic alloy.

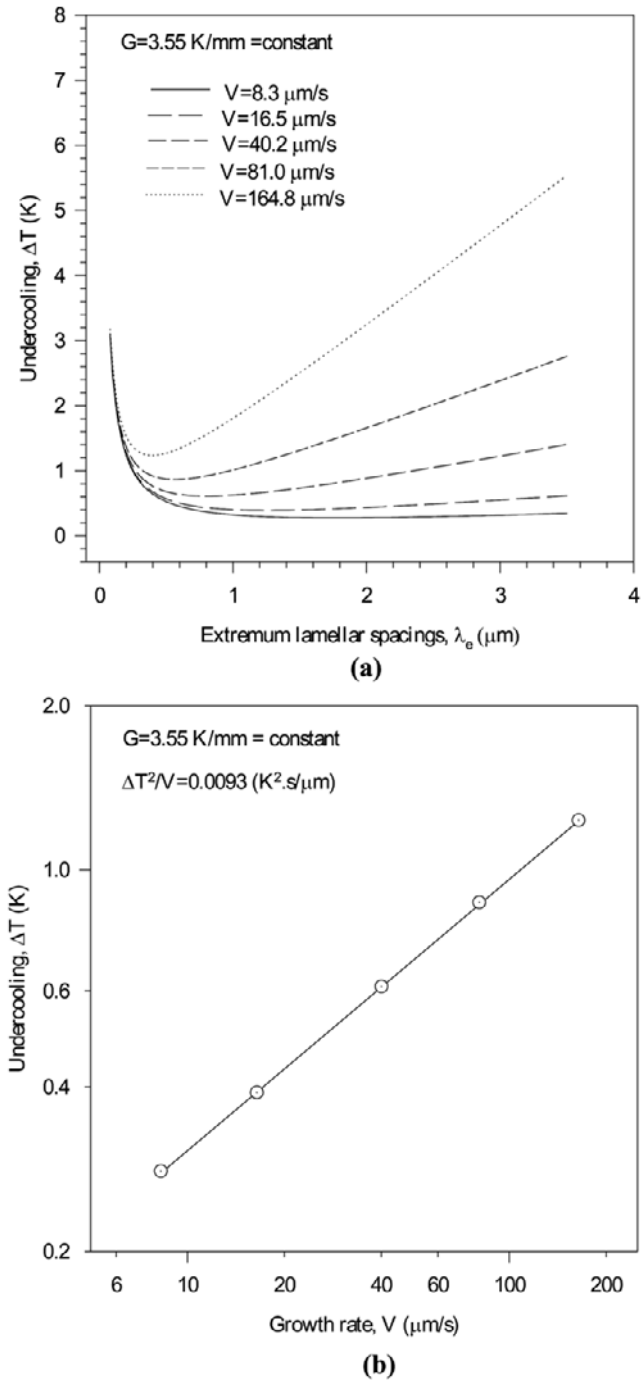

Fig. 5. (a) Variations of the calculated values of minimum undercooling (ΔT) versus the lamellar spacing (λ) at a constant temperature gradient (G = 3.55 K/mm). (b) The variation of the minimum undercooling (ΔT) as a function of growth rates (V) at a constant temperature gradient (G = 3.55 K/mm).

ity of phases in each phase, the grey phase is the pure Bi phase and the black phase is the Sn solid solution phase.

2.2. The measurements of lamellar spacings, temperature gradient and growth rate

The lamellar spacings (λ_a, λ_a^*, λ_m^* and λ_M^*) were measured from the photographs with a linear intercept method [24]. These spacings were measured from transverse and longitudinal sections. The values of λ_a, λ_a^*, λ_m^* and λ_M^* are given in Table 2 and shown in Fig. 4 as a functions of V at a constant

G. K-type thermocouples were used for measurement of temperature gradient and growth rate during solidification. All the thermocouple leads were taken to the data-logger and the computer [49]. The thermocouples were both recorded simultaneously for measurement of the temperature gradients on the solid/liquid interface in the liquid by means of the data-logger. The details of measurements of G and V are given in refs [7,23,30-32].

2.3. The determination of minimum undercooling (ΔT_m)

If the values of K_1 and K_2 are known or calculated from phase diagram and growth rate (V) and the extremum lamellar spacing (λ_e) measured, then the value of the extremum undercooling (ΔT_e) can be determined from Eqs. 6(b) and (c). The minimum undercooling values (ΔT_m) for Bi- 43 wt.% Sn eutectic alloy were obtained from Eqs. 6(b) and (c); the detailed ΔT-λ curves are shown in Fig. 5; these curves were plotted by using experimental V and G values with the system parameters K_1 and K_2.

2.4. The measurement of microhardness, H_v

Microhardness measurements were made with a standardized Vickers indenter using a 25 g load and a dwell time of 10 s by using Fujitech FM-700 model hardness measuring test device. The microhardness was the average of at least ten measurements on the transverse section ($H_{V(tr)}$) and the longitudinal section ($H_{V(long)}$), as shown in Fig. 6. The minimum impression spacing (the centre to the edge of adjacent impression) was about three times the diagonal and at least 0.5 mm from the edge of the sample. The values of λ, V and H_V are given in Table 2.

3. RESULT AND DISCUSSION

In order to see the effect of growth rates (V) on the lamellar spacings (λ) and the undercooling (ΔT) in Sn-Bi eutectic system, the samples were unidirectionally solidified with different growth rates (8.3 μm/s to164.8 μm/s) at a constant temperature gradient (3.55 K/mm). As can be seen from Figs. 2 and 3, a large number of eutectic grains can be formed during eutectic growth. All grains seem to be oriented parallel to growth direction but usually differ in rotation about the growth axis. The normal of the α and β planes must be parallel to the polished longitudinal plane [23]; however, this situation is not always possible. When the normals of the α and β planes are not parallel to the longitudinal plane, the lamellar spacings λ^* observed on the longitudinal plane give larger value than the lamellar spacings λ from the transverse

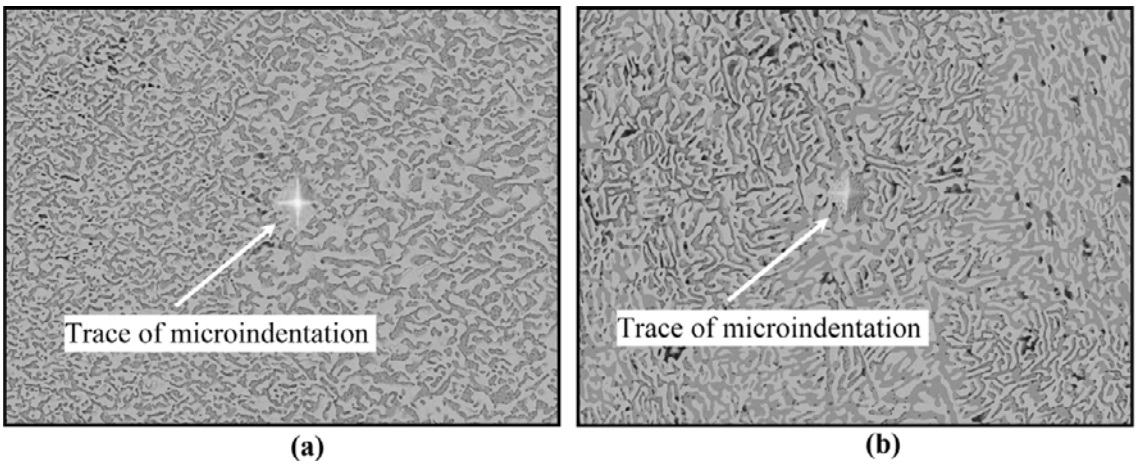

Fig. 6. Optical microscopy images of microindentation traces of directionally solidified Bi- 43 weight pct Sn eutectic samples, (a) from longitudinal section (b) from transverse section.

Table 2. The values of lamellar spacings (λ), growth rate (V), undecooling (ΔT) and microhardness (H_V) for the directionally solidified Bi-43 weight pct Sn eutectic alloy at a constant temperature gradient (G = 3.55 K/mm)

Solidification parameters			Lamellar spacings					Microhardness	
G (K/mm)	V (μm/s)	ΔT (K)	λ_e (μm)	λ_a (μm)	λ_a^* (μm)	λ_m^* (μm)	λ_M^* (μm)	$H_{V(tr)}$ (kg/mm^2)	$H_{V(long)}$ (kg/mm^2)
3.55	8.3	0.28	1.76±0.15	1.90±0.17	2.45±0.22	2.12±0.20	2.84±0.26	18.5	17.8
	16.5	0.39	1.25±0.13	1.48±0.15	1.97±0.18	1.67±0.14	2.15±0.20	20.1	19.4
	40.2	0.61	0.80±0.09	0.94±0.10	1.24±0.13	1.06±0.09	1.60±0.14	22.4	21.3
	81.0	0.87	0.56±0.06	0.66±0.07	0.90±0.08	0.78±0.06	1.13±0.10	24.2	22.6
	164.8	1.23	0.40±0.03	0.44±0.04	0.58±0.05	0.47±0.04	0.76±0.06	26.6	24.8

λ: The values of the lamellar spacing obtained from the transverse section of the samples.
λ^*: The values of the lamellar spacing obtained from the longitudinal section of the samples.

Table 3. The values of growth rate (V), temperature gradient (G) and lamellar spacing (λ), for directionally solidified some metallic alloy with different growth conditions and the experimental relationships between them

Alloy	T_E (K)	G (K/mm)	V (μm/s)	λ (μm)	Relationships λ^2V (μm^3/s) $\Delta T^2/V$(K^2·s/μm) $\lambda_a\Delta T$ (K·μm)	Ref.
Sn-Bi eutectic	412	3.55	8.3-164.8	0.44-1.90	λ^2V=33.76 $\Delta T^2/V$=0.0093 $\lambda_a\Delta T$=0.56	This work
					λ^2V=25.80	J-H Theory
Cd-Sn eutectic	449	4.38.	1-165	0.51-2.19	λ^2V=44.02 $\Delta T^2/V$=0.020 $\lambda_a\Delta T$=0.96	[49]
Cd-Sn eutectic	449	12.0	3-14	1.6-3.4	λ^2V=34.6	[54]
Cd-Sn eutectic	449	2.0	7-84	0.64-2.22	λ^2V=34.7 $\Delta T^2/V$=0.017	[55]
Al-Cu eutectic	821	2.0	7-84	1.10-3.84	λ^2V=103.0 $\Delta T^2/V$=0.016	[55]
Bi-Cd eutectic	418	1.9-4.78	.3-167.3	0.50-3.15	λ^2V=39.06 $\Delta T^2/V$=0.0027 $\lambda_a\Delta T$=0.32	[57]
Pb-Sn eutectic	456	-	0.5-50	0.55-5.4	λ^2V=14.6	[28]
Pb-Sn eutectic	456	1.1-4.7	9.6-144.9	0.49-1.90	λ^2V=35.1	[7]
Sn-Zn eutectic	471	6.58.	3-165.1	0.50-2.21	λ^2V=40.6 ΔT^2V=0.0072 $\lambda_a\Delta T$=0.529	[32]
Pb-Cd eutectic	521	6.4	8.3-163.5	0.38-1.69	λ^2V=23.7 ΔT^2V=0.063 $\lambda_a\Delta T$=1.13	[31]
Pb-Cd eutectic	521	7.3-10.9	0.36-13700	0.042-8.5	λ^2V=21.1	[18]
Pb-Cd eutectic	521	-	-	-	λ^2V=21.8 ΔT^2V=0.0022	[25]
Al-Cu eutectic	821	18.5-26.0	1.1-25	1.82-8.68	λ^2V=83.0	[56]
Pb-Sn eutectic	456	10.0-15.0	6-17	1.41-2.37	λ^2V=33.8	[56]
Al-Cu eutectic	821	5.8-38.0	9.5-483.2	0.57-4.04	λ^2V= 156.0	[23]
Al-Cu eutectic	821	7.6	21.6-432	0.62-2.75	λ^2V=164.0	[24]

polished plane [49]. As can be seen in Table 2, even some of the λ_m^* values can be higher than the average λ_a values. From a longitudinal view, the lamellar spacing seems to be different in each grain because grains were cut under different angles θ to the polished surface. The value of θ_a was obtained to be $40.9^o\pm1.3^o$ by using the measured values of λ_a^* and λ_a, which are given in Table 2. For that reason, longitudinal sections are inadequate for evaluation of the lamellar spacing without geometrical correction. It was observed that the values of λ_a measured on the transverse section of the sample are more reliable. In this work, the values of λ_a have been compared with those of the J-H theory and with the previous results [7,18,23,25,26,31,32] and the comparison is given in Table 3.

For eutectic and near-eutectic composition alloys, the fluid-flow effect is negligible [27]. Although fluid-flow does not exist in thin samples (<1 mm I.D.), its effect is small in the bulk samples. Because the density of the liquid also depends on the solute concentration, the rejection of solute modifies the density field within the solute layer. If the solute layer is heavier than the solvent (as in Sn-Bi) then both the solutal and thermal buoyancy forces are parallel to the gravity vector. Under this ideal case of no horizontal variation of temperature, this arrangement is hydrostatically stable (*i.e.*, fluid motion is negligible), and the transport of solute must be solely due to molecular diffusion along the growth direction [27]. The inner diameter of the crucible used in the present work is 4 mm. So, the fluid-flow effect on the lamellar eutectic is negligible.

In addition to the above microstructural characteristics, several solidification faults like layer mismatches and lamellar termination were observed. As can be seen in Fig. 1(b),

Table 4. The relationships between growth rate, lamellar spacings and undercooling for the Bi- 43 wt.% Sn eutectic alloy solidified with different growth rates at a constant temperature gradient (G = 3.55 K/mm). The undercooling (ΔT) was calculated from eutectic theory (Eq. 6) by using the experimental values of V and λ

$\lambda_e\Delta T$ (Kμm)	$\lambda_a\Delta T$ (Kμm)	$\lambda_a^*\Delta T$ (Kμm)	$\lambda_m^*\Delta T$ (Kμm)	$\lambda_M\Delta T$ (Kμm)	$\lambda_e^2 V$ ($\mu m^3/s$)	$\lambda_a^2 V$ ($\mu m^3/s$)	$\lambda_a^{2*} V$ ($\mu m^3/s$)	$\lambda_m^{2*} V$ ($\mu m^3/s$)	$\lambda_M^{2*} V$ ($\mu m^3/s$)	$\Delta T^2/V$ ($K^2\cdot s/\mu m$)
0.49	0.53	0.69	0.59	0.80	25.71	29.96	49.93	37.30	66.94	0.0094
0.49	0.58	0.77	0.65	0.84	25.78	36.14	64.03	46.02	76.27	0.0092
0.49	0.57	0.76	0.65	0.98	25.73	35.52	61.81	45.17	102.91	0.0093
0.49	0.57	0.778	0.68	0.98	25.40	35.28	65.61	49.28	103.43	0.0093
0.49	0.54	0.71	0.68	0.93	26.37	31.91	55.44	36.40	95.19	0.0092
0.49	0.56	0.74	0.63	0.91	25.80	33.76	59.34	42.83	88.95	0.0093

The bold values are averaged values.
*calculated from J-H theoretical model

the α-β boundary tilts toward the β lamella side and α pocked range will appear in the liquid in the front of the α-L interface with finally a new β lamella growing in the pocked range and a positive termination forming. Through this dynamic mechanism, the local spacing will decrease (λ_m^*). The α-β boundary tilts toward the α lamella side and the local α-L interface disappears with the α lamella being overlapped by two neighboring β lamella (a negative termination) [20-22]. Despite this microstructure, which changed by positive and negative termination mechanism, the values of λ_m^* and λ_M^* were measured as closely as possible on each specimen.

The measured values of lamellar spacings (λ), growth rate (V), undecooling (ΔT) and microhardness (H_V) for the directionally solidified Bi- 43 wt.% Sn eutectic alloy at a constant temperature gradient (G = 3.55 K/mm) are given in Table 2 and the experimental relationships among them are given in Table 4. The dependence of the lamellar spacings (λ), the undecooling (ΔT) and the microhardness (H_V) on the growth rate (V) and the dependence of the microhardness (H_V) on the lamellar spacings (λ) is given in Table 5 for the directionally solidified Bi- 43 wt.% Sn eutectic alloy at a constant temperature gradient (G = 3.55 K/mm).

3.1. The effect of the growth rate on the lamellar spacings

Variations in lamellar spacings (λ) with growth rates (V) at a constant temperature gradient (G = 3.55 K/mm) are given in Table 2 and shown in Fig. 4(a). The variation of lamellar spacings versus growth rate is essentially linear on the logarithmic scale. As can be seen in Table 2 and Figs. 4(a) and (b), the data form straight lines; the linear regression analysis gives the proportionality equation as,

$$\lambda = k_2 V^{-n} \quad \text{(for the constant G)} \tag{9}$$

As can be seen in Table 5, the values of exponent relating to the growth rate for λ_e, λ_a, λ_a^*, λ_m^* and λ_M^* are equal to 0.50, 0.49, 0.47, 0.48 and 0.43 respectively. It is apparent that the dependence of λ values on the growth rate is exponent ional

Table 5. The values of lamellar spacings (λ), growth rate (V), undecooling (ΔT) and microhardness (H_V) for the directionally solidified Bi- 43 wt.% Sn eutectic alloy at a constant temperature gradient (G = 3.55 K/mm) and the experimental relationships between them

The relationships	Constant (k)	Correlation coefficients (r)
$\Delta T=k_1 V^{0.50}$	$k_1=0.097(K\cdot\mu m^{-0.50}\cdot s^{0.50})$	$r_1 = 0.999$
$\lambda_e=k_2 V^{-0.50}$	$k_2=5.04\ (\mu m^{1.50}\cdot s^{-0.50})$	$r_2 = -0.999$
$\lambda_a=k_3 V^{-0.49}$	$k_3=9.54\ (\mu m^{1.49}\cdot s^{-0.49})$	$r_3 = -0.997$
$\lambda_a^*=k_4 V^{-0.47}$	$k_4=12.30\ (\mu m^{1.47}\cdot s^{-0.47})$	$r_4 = -0.994$
$\lambda_m^*=k_5 V^{-0.48}$	$k_5=10.96\ (\mu m^{1.48}\cdot s^{-0.48})$	$r_5 = -0.992$
$\lambda_M^*=k_6 V^{-0.43}$	$k_6=12.4\ (\mu m^{1.43}\cdot s^{-0.43})$	$r_6 = -0.985$
$H_{V(tr)}=k_7 V^{0.12}$	$k_7=32.94\ (kg.mm^{-2.12}.s^{0.12})$	$r_7 = 0.998$
$H_{V(tr)}=k_8\lambda_a^{-0.24}$	$k_8=4.07\ (kg.mm^{-1.76})$	$r_8 = -0.998$
$H_{V(long)}=k_9 V^{0.11}$	$k_9=30.13\ (kg.mm^{-2.11}.s^{0.11})$	$r_9 = 0.993$
$H_{V(long)}=k_{10}(\lambda_a^*)^{-0.22}$	$k_{10}=4.82\ (kg.mm^{-1.78})$	$r_{10} = -0.993$

and the average value of exponent relating to the growth rate was found to be 0.47 that is close to 0.50 predicted by J-H eutectic theory. This exponent value (-0.47) is in a good agreement with the values of -0.50 and -0.52 obtained by Liu [51] for Pb-Sn eutectic system and Ravishangar *et al.* [52] for MnBi-Bi eutectic system but it is smaller than value of -0.66 obtained by Baragor *et al.* [53] for Bi-Pb eutectic.

As can be seen in Table 4, the experimental measurements in the Sn-Bi eutectic system obey the relationships $\lambda^2 V$ = constant at a constant temperature gradient (G = 3.55 K/mm), {$\lambda_e^2 V$ 25.80 $\mu m^3/s$ (calc.), $\lambda_a^2 V$ = 33.76 $\mu m^3/s$, $\lambda_e^{2*} V$ = 59.34 $\mu m^3/s$, $\lambda_m^{2*} V$ = 42.83 $\mu m^3/s$, $\lambda_M^{2*} V$ = 88.95 $\mu m^3/s$}. The experimental value of $\lambda^2 V$ = 33.76 is very close to the theoretical value of $\lambda^2 V$ = 25.80 calculated from J-H eutectic theory.

The value of $\lambda^2 V$ = 33.76 $\mu m^3/s$ is very close to the values of 34.6 $\mu m^3/s$, 34.7 $\mu m^3/s$, 33.8 $\mu m^3/s$, 35.10 $\mu m^3/s$, 40.61 $\mu m^3/s$ and 39.06 $\mu m^3/s$ obtained by Clark and Elliott [54] and Borland and Elliott [55] for the Cd-Sn eutectic system, Jordan and Hunt [56] and Çadırlı and Gündüz [7] for the Pb-Sn eutectic system, and Kaya et al. [32,57] for the Sn-Zn and the Bi-Cd eutectic systems, respectively.

The value of $\lambda_a^2 V = 33.76\ \mu m^3/s$ is slightly higher than the values of 21.1 $\mu m^3/s$, 21.8 $\mu m^3/s$, 23.7 $\mu m^3/s$ and 19.6 $\mu m^3/s$ obtained by Trivedi *et al.* [18], Moore and Elliot [25] and Çadırlı et al.[31] for the Pb-Cd eutectic system, and Whelan and Haworth [33] for the Bi-Cd eutectic system, respectively. The value of $\lambda_a^2 V = 33.02\ \mu m^3/s$ is fairly smaller than the value of 156 $\mu m^3/s$ obtained by Çadırlı *et al.* [23] for the Al-Cu eutectic. As can be seen from these results and from the information in Table 4, the values of $\lambda^2 V$ obtained in the present work are closer to the values of $\lambda^2 V$ obtained in previous experimental works for Cd-Sn, Pb-Sn, Sn-Zn, Bi-Cd eutectic systems except for the value for the Al-Cu eutectic system. So, $\lambda^2 V$ values might be dependent on components of the eutectic systems.

3.2. Effect of growth rate on the minimum undercooling

Figure 5 shows the minimum undercooling (ΔT) of the solidifying interface. This value was obtained from Eq. 6(c) and the ΔT-λ curves that were plotted by using the experimental values of V and G. Figure 5(a) shows the relationship between ΔT and λ for the Sn-Bi eutectic alloy solidified with different growth rates (V) at a constant temperature gradient (G = 3.55 K/mm). As can be seen from Fig. 5(a), the influence of V on the lamellar spacings (λ) and the undercooling (ΔT) is certain. The value of ΔT increases with the increasing value of V, whereas λ_e decreases with the increasing value of V. Although V values increased approximately 20 times, ΔT value increased approximately 4.5 times.

Figure 5(b) shows the variation of ΔT as a function of V in a constant G. ΔT increases with the increasing V. As can be seen in Table 4 and in Fig. 5(b), the dependence of ΔT on V and λ can be given as

$$\Delta T^2/V = 0.0093\ (K^2 \cdot s/m) \quad \text{(for the constant G)} \qquad (10(a))$$

$$\lambda_a \Delta T = 0.56\ (K\ \mu m) \text{ (for the constant G)} \qquad (10(b))$$

The exponent value of growth rate (0.50) is in a good agreement with the values of 0.53, 0.48, 0.50, 0.56, 0.50 and 0.50 obtained by Gündüz *et al.* [30] for Al-Si eutectic alloy, Çadırlı *et al.* [31] for Pb-Cd eutectic alloy, Kaya *et al.* [32,57] for Sn-Zn and Bi-Cd eutectic alloys, and Çadırlı *et al.* [49] for Sn-Cd eutectic alloy and J-H eutectic theory, respectively.

The value (0.0093) is slightly smaller than the value 0.017 obtained by Borland and Elliott [55] for the same alloy system. The values of $\lambda_a \Delta T = 0.56$ and $\Delta T^2/V = 0.0093$ are in a good agreement with values of $\lambda_a \Delta T = 0.53$ and $\Delta T^2/V = 0.0072$ obtained by Kaya *et al.* [32] for the Sn-Zn eutectic system. Also, the same values are lower than the values of $\lambda_a \Delta T = 1.134$ and $\Delta T^2/V = 0.054$ obtained by Çadırlı *et al.* [31] for the Pb-Cd eutectic. These discrepancies in the values of $\Delta T^2/V$ and $\lambda_a \Delta T$ might be because of the components of eutectic systems.

3.3. Influence of growth rate or lamellar spacing on the microhardness

Table 2 and Fig. 7(a) show the variations of microhardness (H_V) as a function of growth rate (V) at a constant temperature gradient (G = 3.55 K/mm). The value of H_V increases

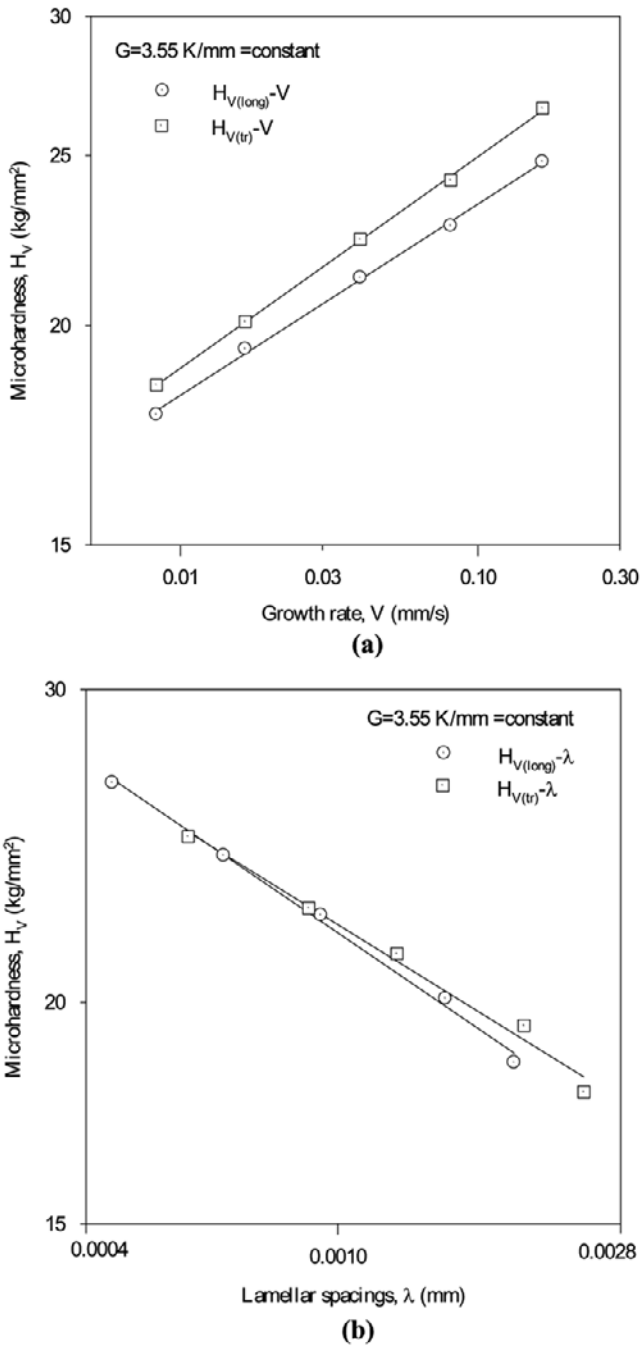

Fig. 7. (a) Variation of the microhardness (H_V) as a function of (a) growth rate (V), (b) lamellar spacing (λ) for directionally solidified Bi- 43 weight pct Sn eutectic alloy with different growth rates (8.3 μm/s to 164.8 μm/s) in a constant temperature gradient (G = 3.55 K/mm).

with the increasing value of V. As can be seen in Table 5, the exponent values of m that relate to growth rate are equal to 0.12 and 0.11 for the transverse and longitudinal sections of the Sn-Bi eutectic alloy, respectively. These exponent values have been compared with those found in the previous results [58-65] for similar solidification conditions in different eutectic alloys. The exponent values of m obtained in the present work are fairly close to the values 0.12, 0.07, 0.08, 0.10, 0.11, 0.14 and 0.10 of m obtained by Khan *et al.* [58], Vnuk *et al.* [59], Telli and Kısakürek [60], Kaya *et al.* [35,61], Lapin *et al.* [62] and Vnuk *et al.* [63] for different eutectic alloy systems, respectively. Our exponent values of m are rather higher than the values of 0.04, and 0.034, obtained for the Al-Si eutectic alloys by Yılmaz and Elliot [64] and Yılmaz [65], respectively.

As can be seen in Table 2 and in Fig. 7(b), the values of H_V decrease with the increasing values of λ in a constant temperature gradient, G. Dependence of microhardness on the growth rates and lamellar spacing is given in Table 5. The exponent values of n, which is related to lamellar spacing, λ, are equal to 0.24 and 0.22 for the transverse and longitudinal sections of the same eutectic alloy. These values of n are in the good agreement with the values of 0.22, 0.18 and 0.22 obtained by Khan *et al.* [58] and Kaya *et al*. [35,61], but higher than the value of 0.08 obtained by Yılmaz and Eliot [64], and do not confirm the value of 0.5 suggested by Telli and Kısakürek [60] for Al-Si eutectic alloys.

4. CONCLUSIONS

The lamellar spacing is strongly dependent on the growth rate, since an increase in growth rate causes microstructure refinement, which is shown in Table 2. At 3.55 K/mm temperature gradient, the highest and the smallest lamellar spacings were obtained with 8.3 μm/s and 164.8 μm/s growth rates, as shown in Figs. 4(a), 4(b), 3(e), and 3(f), respectively. Lamellar spacings decrease inversely as the square root of the growth rate for directionally solidified Bi- 43 wt.% Sn alloy with different growth rates (8.3 μm/s to 164.8 μm/s) at a constant temperature gradient (G = 3.55 K/mm). The relationships between these values were obtained by binary regression analysis as follows:

$$\lambda_a = k_3 V^{0.49} \text{ (where the value of } k_3 \text{ is equal to } 9.54\ \mu m^{1.49}.s^{-0.49})$$

This exponent value is in a good agreement with that in the J-H eutectic theory [11] and with that found in some other experimental works [51,52].

By using experimental values of λ_a and V, the bulk growth rate ($\lambda_a^2 V$) was found to be 33.76 $\mu m^3/s$. The value of bulk growth rate determined is slightly higher than the calculated value 25.80 $\mu m^3/s$ from the J-H theoretical approach but is in a good agreement with the values found in some other experimental studies [7,32,54-56].

Effect of growth rate, V on the undercooling, ΔT, at a constant temperature gradient was examined and the relationship between these factors was found to be $\Delta T^2/V=0.0093$ $K^2.s/mm$. The constant value, 0.0093, is slightly smaller than the value 0.017 obtained by Borland and Elliott [55] for the same alloy system.

The minimum undercooling (ΔT) increases with the increasing growth rate (V) for a given temperature gradient (G), whereas the extremum lamellar spacing (λ_e) decreases. On the other hand, the value of $\lambda_a \Delta T$ was found to be 0.56 Kμm, which is fairly close to some other results in the literature [31,32].

The values of microhardness (H_V) for directionally solidified Bi- 43 wt.% Sn eutectic alloy at a constant temperature gradient (G = 3.55 K/mm) increase with the increasing value of growth rates (V) and decreasing value of lamellar spacing (λ); the relationships between these factors has been found to be $H_V = kV^{0.11}$ ($k = 30.13\ kg.mm^{-2.11}.s^{0.11}$) and $H_V = k\lambda^{-0.22}$ ($k = 4.82\ kg.mm^{-1.78}$). These exponent values are in a good agreement with those of the previous experimental works [35,58-63].

ACKNOWLEDGMENT

This project was supported by the State Planning Organization of Turkey (2003K 120880-4). The authors would like to thank the State Planning Organization of Turkey for its financial support.

REFERENCES

1. R. Elliott, *Eutectic Solidification Processing Crystalline and Glassy Alloys*, p. 58, Butterworths, UK (1983).
2. M. McLean, *Directionally Solidified Materials for High Temperature Service*, p. 107, The Metal Society Book, London (1983).
3. D. M. Stefanescu, G. J. Abbaschian, and R. J. Bayuzick, *Solidification Processing of Eutectic Alloy*, p. 85, American Society for Metals, OH (1988).
4. M. C. Flemings, *Solidification Processing*, p. 280, Mc Graw Hill, NewYork (1974).
5. J. M. Liu, Y. Zhou, and B. Shang, *Acta metall.* **38**, 1625 (1990).
6. P. Magnin, J. T. Mason and R. Trivedi, *Acta metall.* **39**, 469 (1991).
7. E. Çadırlı and M. Gündüz, *J. Mat. Proceess. Tech.* **97**, 74 (2000).
8. Y. X. Zhuang, X. M. Zhang, L. H. Zhu, and Z. Q. Hu, *Sci. Tech. Adv. Mat.* **2**, 37 (2001).
9. J. D. Hunt, *Sci. Tech. Adv. Mat.* **2**,147 (2001).
10. Y. J. Chen, S. H. Davis, *Acta metall.* **50**, 2269 (2002).
11. K. A. Jackson, J. D. Hunt, *Metall. Soc. A.I.M.E.* **236**, 1129

(1966).
12. R. Trivedi, P. Magnin, and W. Kurz, *Acta metall.* **35**, 971 (1987).
13. R. M. Jordan and J. D. Hunt, *J. Cryst. Growth* **11**, 141 (1971).
14. P. Magnin and W. Kurz, *Acta metall.* **35**, 1119 (1987).
15. P. Magnin and R. Trivedi, *Acta metall.* **39**, 453 (1991).
16. W. Kurz and R. Trivedi, *Metall. Trans. A* **22**, 3051 (1991).
17. V. Seetharaman and R. Trivedi, *Metall. Trans. A* **19**, 2955 (1988).
18. R. Trivedi, J. T. Mason, J. D. Verhoeven, and W. Kurz, *Metall. Trans. A* **22**, 2523 (1991).
19. G. H. Nash, *J. Cryst. Growth* **38**, 155 (1977).
20. G. Sharma, R. V. Ramanujan, and G. P. Tivari, *Acta mater.* **48**, 875 (2000).
21. J. M. Liu, *Mat. Sci. Eng. A* **157**, 73 (1992).
22. J. M. Liu, Z. C. Wu, and Z. G. Liu, *Scripta metall.* **27**, 715 (1992).
23. E. Çadırlı, A. Ülgen, and M.Gündüz, *Mater. Trans. (JIM)* **40**, 989 (1999).
24. A. Ourdjini, J. Liu, and R. Elliott, *Mater. Sci. Tech.* **10**, 312 (1994).
25. A. Moore and R. Elliott, *The Solidification of Metals, Joint Conference*, p. 100, Iron Steel Ins. Publ., Brighton (1969).
26. H. Cline, *Mat. Sci. Eng.* **65**, 93 (1984).
27. J. J.Favier and J. De Goer, *Results Spacelab I*, p. 127, ESA SP-222, European Space Agency Special Publications, Paris (1984).
28. J. Liu and R. Elliott, *Metall. Trans. A* **26**, 471 (1995).
29. K. Kassner and C. Misbah, *Phys. Rev. A* **44**, 6533 (1991).
30. M. Gündüz, H. Kaya, E. Çadırlı, and A. Özmen, *Mat. Sci. Eng. A* **369**, 215 (2004).
31. E. Çadırlı, H. Kaya, and M. Gündüz, *Mat. Res. Bull.* **38**, 1457 (2003).
32. H. Kaya, E. Çadırlı, and M. Gündüz, *J. Mat. Eng. Perf.* **12**, 465 (2003).
33. E. P. Whelan and C. W. Haworth, *J. Aust. Inst. Metals* **12**, 77 (1967).
34. W. Kurz and D. J. Fisher, *Acta metall.* **28**, 777 (1980).
35. H. Kaya, M. Gündüz, E. Çadırlı, and O. Uzun, *J. Mat. Sci.* **39**, 6571 (2004).
36. *Metals Handbook, 8th ed., Vol. 8* (ed., T. Lyman), p. 86, American Society for Metals, Metals Park, OH (1973).
37. B. Saatci, *Ph. D.Thesis*, University of Erciyes, Kayseri, Turkey (2000).
38. M. Erol, N. Maraşlı, K. Keşlioğlu, and M.Gündüz, *Scripta metall.* **51**, 131 (2004).
39. M. V. Hecht and H. W.Kerr, *J. Cryst. Growth* **7**, 136 (1970).
40. V. Datye and J. S. Langer, *Phys. Rev. B* **24**, 4155 (1981).
41. A. Munitz, *Metall. Trans. B* **16**, 149 (1985).
42. M. Zimmermann, M. Carrard, and W. Kurz, *Acta metall.* **37**, 3305 (1989).
43. N. Cheung, M. C. Ierardi, A. Garcia, and R. Vilar, Lasers Eng. **10**, 275 (2000).
44. W. R. Osório and A. Garcia, *Mater. Sci. Eng. A* **325**, 104 (2002).
45. J. M. Quaresma, C. A. Santos, and A. Garcia, *Metall. Mater. Trans. A* **31**, 3167 (2000).
46. C. Siqueira, N. Cheung and A. Garcia, *Metall. Mater. Trans. A* **33**, 2107 (2002).
47. E. O. Hall, *Proc. Phys. Soc. B.* **64**, 747 (1957).
48. N. J. Petch, *J. Iron Steel Inst.* **174**, 25 (1953).
49. E. Çadırlı, H. Kaya, and M.,Gündüz,*J. Alloy. Compd.* **431**, 171 (2007).
50. M. Hansen and K. Anderko, *Constitutions of Binary Alloys*, p. 303, McGraw-Hill, New York (1958).
51. J. M. Liu, *Scripta metall.* **26**, 179 (1992).
52. P. S. Ravishankar, W. R. Wilcox, and D. J. Larson, *Acta metall.* **28**, 1583 (1980).
53. D. Baragor, M. Sahoo, and R. W. Smith, *Solidification and Casting of Metals*, p. 88, The Metal Society, London (1979).
54. J. N. Clark and R. Elliott, J. Cryst. Growth **33**, 169 (1976).
55. S. M. D. Borland and R. Elliott, *Metall. Trans. A* **9**, 1063 (1978).
56. R. M. Jordan and J. D. Hunt, *Metall. Trans.* **2**, 3401 (1971).
57. H. Kaya, E. Çadırlı, and M. Gündüz, *J. Mat. Process. Tech.* **183**, 310 (2007).
58. S. Khan, A. Ourdjini, Q. S. Hamed, M. A. A.Najafabadi, and R. Elliott, *J. Mat. Sci.* **28**, 5957 (1993).
59. F. Vnuk, M. Sahoo, R. Van De Merve, and R. W. Smith, *J. Mat. Sci.* **14**, 975 (1979).
60. A. I. Telli and S. E. Kısakürek, *Mat. Sci. Tech.* **4**, 153 (1988).
61. H. Kaya, E. Çadırlı, M. Gündüz, and A. Ülgen, J. Mat. Eng. Per. **12**, 544 (2003).
62. J. Lapin, L. Ondrus, and M. Nazmy, *Intermetallics* **10**, 1019 (2002).
63. F. Vnuk, M. Sahoo, D. Baragor, and R. W. Smith, *J. Mat. Sci.* **15**, 2573 (1980).
64. F. Yılmaz and R. Elliott, J. Mat. Sci. **24**, 2065 (1989).
65. F. Yılmaz, *Mat. Sci. Eng. A* **124**, L1 (1990).